Research Article Vol. 34, No. 9 / September 2017 / Journal of the Optical Society of America B 1923

Journal of the Optical Society of America B

OPTICAL PHYSICS

Optical bistability forming due to a Rydberg state

HAMID REZA HAMEDI,[1,*] MOSTAFA SAHRAI,[2] HABIB KHOSHSIMA,[2] AND GEDIMINAS JUZELIŪNAS[1]

[1]Institute of Theoretical Physics and Astronomy, Vilnius University, Sauletekio 3 LT-10222 Vilnius, Lithuania
[2]Research Institute for Applied Physics and Astronomy, University of Tabriz, Tabriz, Iran
*Corresponding author: hamid.hamedi@tfai.vu.lt

Received 27 March 2017; revised 21 July 2017; accepted 23 July 2017; posted 26 July 2017 (Doc. ID 291505); published 17 August 2017

We consider the behavior of optical bistability (OB) and multistability (OM) in a four-level atomic system involving a Rydberg state illuminated by a probe field as well as control and switching laser beams of larger intensity. When the switching field is absent, no OB arises because of the effect of Rydberg electromagnetically induced transparency. However, by application of the switching field, the hysteresis cycle appears to give rise to optical bistability, thanks to Rydberg electromagnetically induced absorption. It is further demonstrated that one can efficiently modify the OB threshold via suitable choices of system-controlling parameters. Interestingly, it is observed that this model can produce an optical switching between OB and OM with potential applications in logic-gate devices for optical communication.

OCIS codes: (190.1450) Bistability; (270.0270) Quantum optics; (020.1670) Coherent optical effects.

https://doi.org/10.1364/JOSAB.34.001923

1. INTRODUCTION

It is well known that light can be slowed down by several orders of magnitude using the technique of electromagnetically induced transparency (EIT) [1]. EIT can be employed to induce transparency for an opaque and resonant medium using quantum interference between the different optical pathways. In this situation, a weak probe beam of light travels slowly in a resonant medium controlled by another laser beam without any significant absorption [1–8]. Because of changing absorption and dispersion characteristics of an atomic medium [9–16], EIT can result in several interesting phenomena in nonlinear optics, such as multiwave mixing [17–20], an enhanced Kerr nonlinearity [21–28], stable optical solitons [29–34], and optical bistability [35–43]. The optical bistability (OB) has been investigated both theoretically and experimentally in various multilevel EIT schemes due to its applications in all-optical transistors, switches, logical gates, and quantum memory [44]. For instance, Yuan *et al.* have theoretically investigated the effect of bright and dark states on vacuum Rabi splitting (VRS) and optical bistability of the multiwave-mixing process in a collective four-level atomic-cavity coupling system [42]. It was demonstrated that VRS and self-Kerr nonlinearity OB can coexist and compete with each other in a cascade relationship. As a result, one can control VRS and OB simultaneously through the dark state in the atomic system. The relationship between OB and VRS as well as the coherence-induced bright state in a cavity–atom composite system has been also investigated very recently [43].

Also, several interesting ideas for OB have been also reported in semiconductor quantum well (QW) structures [45–48]. For instance, Li has investigated theoretically the optical bistability behavior based on intersubband transitions in asymmetric double QWs [45]. Coherent control of OB has also been studied in a triple semiconductor quantum well structure with tunneling-induced interference [46]. Tunneling-induced optical bistability in an asymmetric double quantum well has been reported very recently by Li *et al.* [48]. Apart from solid-state quantum well nanostructures, EIT has been observed for rare-earth-doped crystals, such as $Pr^{3+}:Y_2SiO_5$ [49]. Efficient EIT in such solid crystals opens potential applications, such as light storage [50], large refractive index without absorption [51], and coherent control of OB [52]. The generation of twin beams by the parametric amplification four-wave-mixing process and triplet beams by the parametric amplification six-wave-mixing (PA SWM) process associated with the multiorder fluorescence signals in a $Pr^{3+}:Y_2SiO_5$ crystal has been also reported [53].

Using Rydberg atoms, one can apply EIT for nonlinear quantum optics. Because of their extreme polarizability and long-range interactions, Rydberg atoms with highly excited principal quantum numbers [54,55] provide appealing applications in precision electrometry [56] and quantum information [57]. Since the van der Waals interaction between the atoms is enhanced with the principal quantum number, the interaction between the Rydberg atoms is much larger than the interaction between atoms in their ground states [58–60]. Due to the formation of Rydberg dark states in three-level ladder-type atom–light coupling schemes including a Rydberg state, a narrow peak appears in the susceptibility, giving rise to the Rydberg EIT [61–63]. Such a transparency in the medium enables modifications on the refractive index and nonlinear phase shift due to the interactions between particles in the nonlinear processes

0740-3224/17/091923-07 Journal

associated with EIT. Based on this feature, the enhancement and suppression of Rydberg-dressed multiwave-mixing processes with the assistance of EIT windows in a hot Rb atomic system have been investigated both theoretically and experimentally by Zhang *et al.* [64].

As one of its applications, specifically in optical switching, Rydberg electromagnetically induced absorption (Rydberg EIA) can take place instead of the Rydberg EIT by means of coupling of atomic states to other states. An example is the microwave coupling of Rydberg states for which the EIT window is split into a doublet EIT [63].

An interesting issue is to investigate the optical bistability in atomic systems involving a Rydberg state. In doing so, we make use of a four-level atom–light coupling scheme, as shown in Fig. 1, for which EIT/EIA and slow/fast light features have been very recently reported [65–67].

We consider an optical feedback scenario in which the proposed four-level atomic medium with a Rydberg state is placed in a unidirectional ring cavity. Then the dependence of the OB on different system parameters can be explored by plotting the input–output field intensity profile. We show how the OB behavior can be manipulated by means of intensity and detuning of control and switching fields. It is also found that the OB can be converted to the OM via the effect of switching field detuning. Our work may provide significant improvement to the existing studies [35–43] because, to the best of our knowledge, no similar analysis has been done on OB and OB behaviors of atomic ensembles involving a Rydberg state.

2. SYSTEM AND BASIC EQUATIONS

In this section, we shall derive general equations for the propagation of the probe beam in an ensemble of four-level atoms

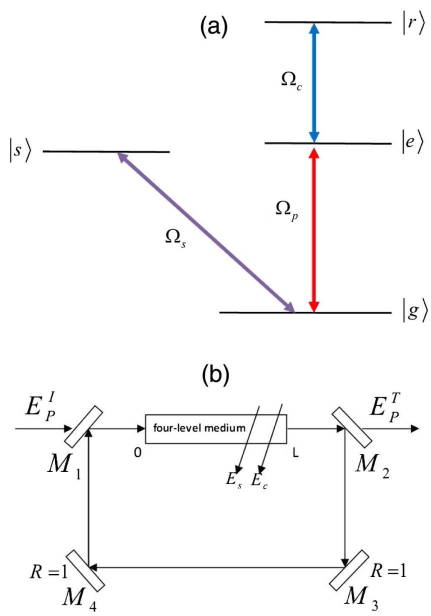

Fig. 1. (a) Four-level atomic system interacting with a probe field Ω_p, a control field Ω_c, as well as a switching field Ω_s. (b) Schematic setup of unidirectional ring cavity containing the proposed medium of length L. Here, E_p^I and E_p^T represent the incident and the transmitted probe fields, respectively.

comprising a Rydberg state, as shown in Fig. 1(a). In this configuration, a ground level $|g\rangle$ is coupled to an intermediate level $|e\rangle$ through a probe field with Rabi frequency Ω_p, and a strong control field Ω_c is employed to mediate the transition $|e\rangle\leftrightarrow|r\rangle$, forming a ladder-type atom–light coupling scheme. The ground level is simultaneously coupled to a level $|s\rangle$ through a switching field Ω_s. Such a scheme can be experimentally implemented using ultracold rubidium atoms in which the level $|g\rangle$ is the $5S_{1/2}$ ground state, the levels $|e\rangle$ and $|s\rangle$ correspond to $5P_{3/2}$ and $5P_{1/2}$ excited states, respectively, while the level $|r\rangle$ is the $44D_{5/2}$ Rydberg state. The decay rates of these states are $\Gamma_g = 0$, $\Gamma_e/2\pi = 6.1$ MHz, $\Gamma_s/2\pi = 5.9$ MHz, and $\Gamma_r/2\pi = 0.3$ MHz.

The total Hamiltonian characterizing the atom-field coupling for the system shown in Fig. 1 is given by ($\hbar = 1$)

$$H_I = (\Delta_p+\Delta_c)|r\rangle\langle r| + \Delta_s|s\rangle\langle s| + \Delta_p|e\rangle\langle e| + \left(\frac{\Omega_p}{2}|g\rangle\langle e| + \frac{\Omega_s}{2}|g\rangle\langle s| + \frac{\Omega_c}{2}|e\rangle\langle r|\right) + \text{h.c.}, \quad (1)$$

where $\Delta_p = \omega_p - \omega_{eg}$, $\Delta_c = \omega_c - \omega_{re}$, and $\Delta_s = \omega_s - \omega_{sg}$ are the corresponding detuning parameters.

Using the susceptibility of the system, one can study the response of the atomic medium due to its interaction with the applied laser fields. In the present situation, the susceptibility is given by

$$\chi = \frac{N\mu_{eg}}{\varepsilon_0 E}\rho_{eg}, \quad (2)$$

where μ_{eg} denotes a dipole matrix element, N is the number density of atoms, and ρ_{eg} is the density matrix element for the probe transition. Density matrix formalism is employed in order to investigate the evolution of the system under consideration

$$\begin{aligned}
\frac{\partial\rho_{eg}}{\partial t} &= \left(-\frac{\Gamma_e}{2}+i\Delta_p\right)\rho_{eg} - \frac{i\Omega_p}{2}(\rho_{ee}-\rho_{gg}) - \frac{i\Omega_s}{2}\rho_{es} + \frac{i\Omega_c}{2}\rho_{rg},\\
\frac{\partial\rho_{sg}}{\partial t} &= \left(-\frac{\Gamma_s}{2}+i\Delta_s\right)\rho_{sg} - \frac{i\Omega_s}{2}(\rho_{ss}-\rho_{gg}) - \frac{i\Omega_p}{2}\rho_{se},\\
\frac{\partial\rho_{rg}}{\partial t} &= \left(-\frac{\Gamma_r}{2}+i(\Delta_p+\Delta_c)\right)\rho_{rg} + \frac{i\Omega_c}{2}\rho_{eg} - \frac{i\Omega_p}{2}\rho_{re} - \frac{i\Omega_s}{2}\rho_{rs},\\
\frac{\partial\rho_{se}}{\partial t} &= \left(-\frac{\Gamma_s+\Gamma_e}{2}+i(\Delta_s-\Delta_p)\right)\rho_{se} + \frac{i\Omega_s}{2}\rho_{ge} - \frac{i\Omega_p}{2}\rho_{sg} - \frac{i\Omega_c}{2}\rho_{sr},\\
\frac{\partial\rho_{re}}{\partial t} &= \left(-\frac{\Gamma_r+\Gamma_e}{2}+i\Delta_c\right)\rho_{re} - \frac{i\Omega_c}{2}(\rho_{rr}-\rho_{ee}) - \frac{i\Omega_p}{2}\rho_{rg},\\
\frac{\partial\rho_{rs}}{\partial t} &= \left(-\frac{\Gamma_r+\Gamma_s}{2}+i(\Delta_p+\Delta_c-\Delta_s)\right)\rho_{rs} + \frac{i\Omega_c}{2}\rho_{es} - \frac{i\Omega_s}{2}\rho_{rg},\\
\frac{\partial\rho_{ee}}{\partial t} &= -\Gamma_e\rho_{ee} + \Gamma_r\rho_{rr} + \frac{i\Omega_p}{2}(\rho_{ge}-\rho_{eg}) + \frac{i\Omega_c}{2}(\rho_{re}-\rho_{er}),\\
\frac{\partial\rho_{ss}}{\partial t} &= -\Gamma_s\rho_{ss} + \frac{i\Omega_s}{2}(\rho_{gs}-\rho_{sg}),\\
\frac{\partial\rho_{rr}}{\partial t} &= -\Gamma_r\rho_{rr} + \frac{i\Omega_c}{2}(\rho_{er}-\rho_{re}), \qquad \rho_{rr}+\rho_{ee}+\rho_{ss}+\rho_{gg}=1,
\end{aligned} \quad (3)$$

where Γ_s, Γ_e, and Γ_r are the decay rates between states $|s\rangle$, $|e\rangle$, and $|r\rangle$ respectively. The decay rate of ground state $|g\rangle$ is considered to be very large compared to other time scales and hence has not been included. According to Eq. (2), we shall find the density matrix element ρ_{eg} in order to trace the atomic response of the system to external fields. Assuming that the atom is initially in its ground level, the steady-state solution for the probe transition reads as

$$\rho_{eg} = \frac{i\Omega_p(x_2\Omega_s^2 + x_4\Omega_c^2 + 4x_2x_3x_4)}{q}, \tag{4}$$

where $q = \Omega_s^2\Omega_c^2 - \Omega_s^4 - \Omega_c^4 - 2\Omega_s^2(x_1x_2 + x_3x_4) - 3\Omega_c^2(x_1x_4 + x_2x_3) - 8x_1x_2x_3x_4$, with $x_1 = -\frac{\Gamma_e}{2} + i\Delta_p$, $x_2 = -\frac{\Gamma_s+\Gamma_e}{2} - i(\Delta_s - \Delta_p)$, $x_3 = -\frac{\Gamma_r+\Gamma_s}{2} + i(\Delta_p + \Delta_c - \Delta_s)$, and $x_4 = -\frac{\Gamma_r}{2} + i(\Delta_p + \Delta_c)$.

3. COHERENT CONTROL OF OPTICAL BISTABILITY

To describe the OB behaviors, the atomic medium of length L is placed in a unidirectional ring cavity, as illustrated in Fig. 1(b). The mirrors 3 and 4 are assumed to be perfect reflectors, whereas the reflection and transmission coefficients of mirrors 1 and 2 are given by R and T, respectively, with $R + T = 1$.

In the steady-state limit, for a perfectly tuned cavity the boundary conditions between the incident field E_1^I and the transmitted field E_1^T are [68]

$$E_1(L) = \frac{E_1^T}{\sqrt{T}}, \tag{5a}$$

$$E_1(0) = \sqrt{T}E_1^I + RE_1(L). \tag{5b}$$

The second term on the right-hand side of Eq. (5b) represents the feedback mechanism stemming from the reflection from the mirrors, which is essential for bistability. By setting $R = 0$ in Eq. (5b), no bistability is expected. According to the mean-field limit and using the boundary conditions, the steady-state behavior of the transmitted field reads as

$$y = 2x - iC\rho_{eg}, \tag{6}$$

where $y = \mu_{eg}E_1^I/\hbar\sqrt{T}$ and $x = \mu_{eg}E_1^T/\hbar\sqrt{T}$ are the normalized input and output fields, respectively. The parameter $C = N\omega_p L|\mu_{eg}|^2/2\hbar\varepsilon_0 cT$ is the cooperatively parameter for atoms in the ring cavity.

We have studied the steady-state behavior of the output field intensity versus the input field intensity for various system parameters. For the resonance condition $\Delta_c = \Delta_s = \Delta_p = 0$ and $\Omega_c = 3\Gamma_e$, the influence of the switching field Ω_s on the behavior of OB is displayed in Fig. 2. It is obvious that no OB can be realized without the switching field (i.e., for $\Omega_s = 0$). Increasing the intensity of the switching field Ω_s, the hysteresis cycle appears to give rise to the optical bistability. With a subsequent growth of Ω_s, the hysteresis cycle becomes larger continually; however, the OB threshold increases only for the range $\Omega_s < \Omega_c$. For $\Omega_s = \Omega_c$, the OB threshold acquires its maximal value. When Ω_s is further increased ($\Omega_s > \Omega_c$), the threshold intensity starts to reduce again. As a result, it is possible to manipulate the OB behaviors through adjusting the switching field intensity.

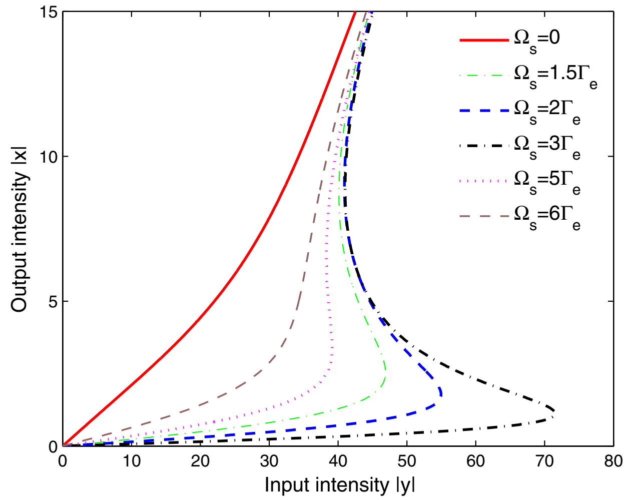

Fig. 2. Plots of the input–output field curves for different values of Ω_s. Here, $\Delta_p = \Delta_s = \Delta_c = 0$, $C = 500\Gamma_e$, $\Omega_c = 3\Gamma_e$, $\Gamma_g = 0$, $\Gamma_e/2\pi = 6.1$ MHz, $\Gamma_s/2\pi = 5.9$ MHz, and $\Gamma_r/2\pi = 0.3$ MHz.

Let us now elucidate such behavior of the optical bistability. Equation (4) of the previous section provides the dependence of probe susceptibility on different controlling parameters of the system. It is well known that the imaginary part of the probe susceptibility is directly related to the probe absorption of the system. The absorption spectrum of the probe laser field is shown in Fig. 3 for the same parametric condition as used in Fig. 2. Note that all the curves are plotted here in units of $\frac{N\mu_{eg}}{\varepsilon_0 E}$. When the switching field is absent ($\Omega_s = 0$), a transparency window appears on resonance, leading to a perfect transmission of the probe laser field [see the solid line in Fig. 3(a)]. This represents the Rydberg EIT in the three-level ladder-type atom–light coupling configuration for which OB does not appear. However, when Ω_s induces the transition $|s\rangle \leftrightarrow |g\rangle$, the Rydberg EIA becomes the dominant mechanism. Working in the Rabi frequency range $\Omega_s < \Omega_c$, four peaks take place in the absorption profile of the system. Simultaneously, the transmission reduces at the line center, as one can see in the dotted and dashed lines in Fig. 3(a). Once the control and switching fields satisfy $\Omega_s = \Omega_c$, the two central absorption peaks join at the line center such that a large absorption occurs, making the medium completely opaque for the probe field tunned to resonance [Fig. 3(b)]. In this case, the OB threshold intensity has its maximum value. Thus, for $\Omega_s \le \Omega_c$, there is a significant increase in the OB threshold in which the cavity field can harder achieve saturation. The probe absorption starts to decrease again for the Rabi frequency range $\Omega_s > \Omega_c$ [Fig. 3(c)], resulting in an enhancement of nonlinearity of the system, which can make the OB threshold reduce significantly. The above discussion also implies that our model can generate an optical switching process between Rydberg EIT and Rydberg EIA in which a transparent medium can be converted to an absorptive one via turning on and off of the switching field Ω_s.

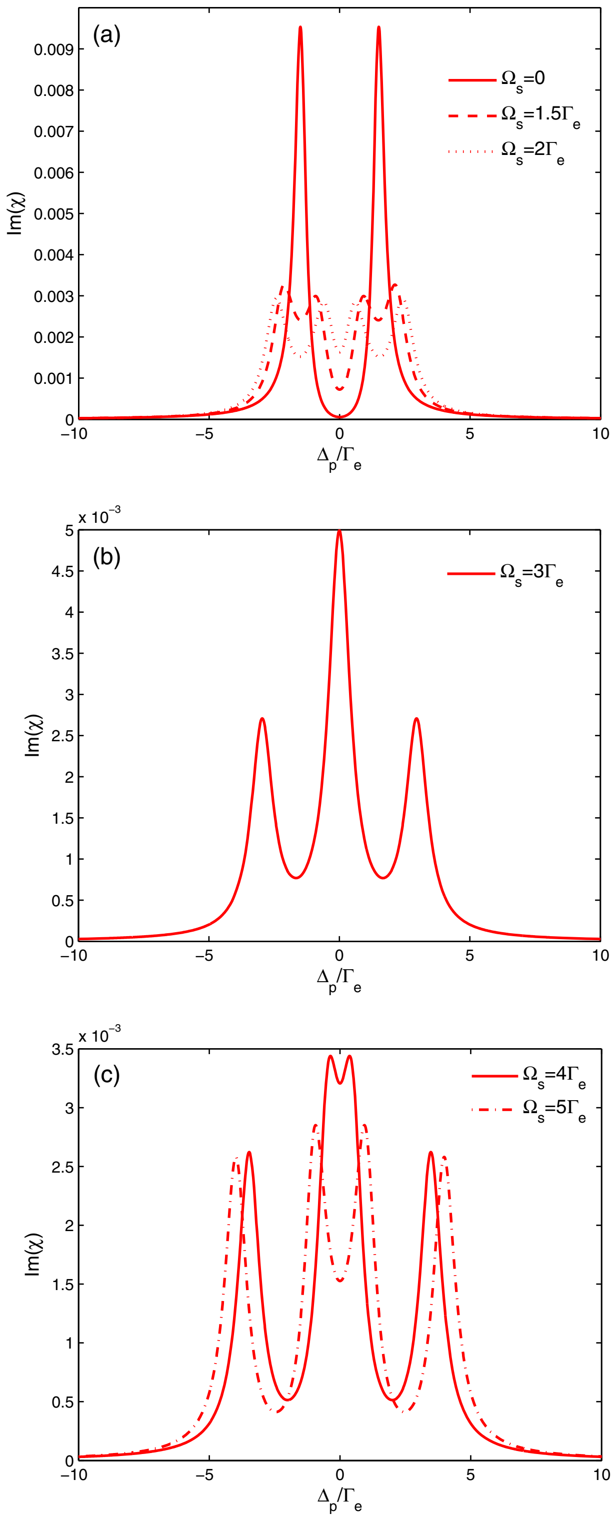

Fig. 3. (a)–(c) Probe absorption versus probe field detuning for different values of Ω_s. Here, $\Omega_p = 0.01\Gamma_e$ and the other parameters are the same as in Fig. 2.

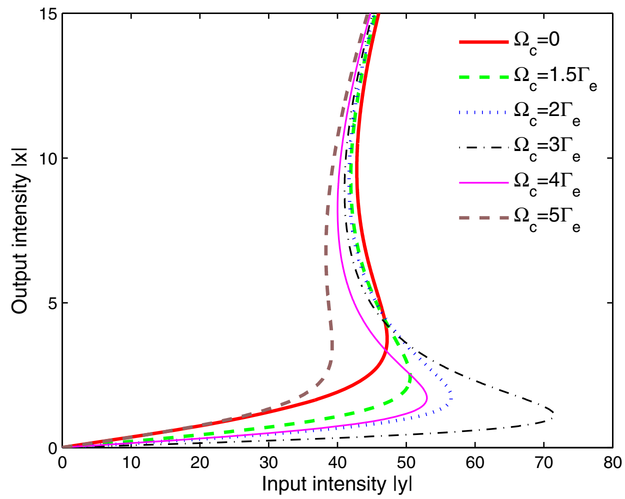

Fig. 4. Plots of the input–output field curves for different values of Ω_c. Here, $\Omega_s = 3\Gamma_e$ and the other parameters are the same as in Fig. 2.

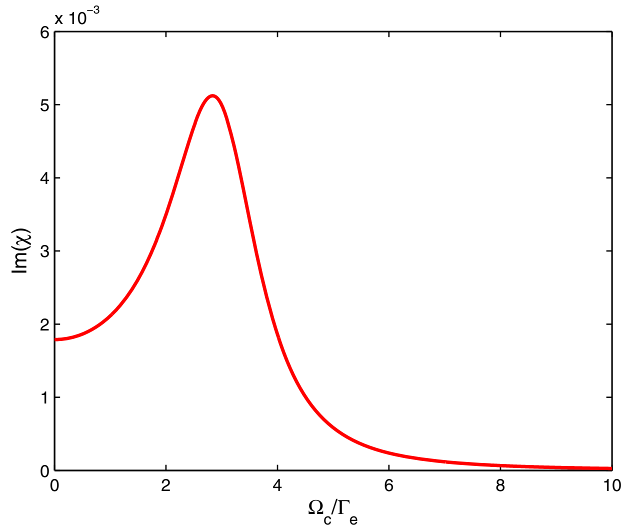

Fig. 5. Probe absorption versus control field Ω_c. Here, $\Omega_p = 0.01\Gamma_e$, $\Omega_s = 3\Gamma_e$ and the other parameters are the same as in Fig. 2.

With the same procedure, we set now $\Omega_s = 3\Gamma_e$ and explore the OB range with changing Ω_c. Figure 4 shows the output versus input probe field in a resonance condition and for different values of Ω_c. One can see that an increase in Ω_c leads to a similar effect on the OB behavior as Ω_s. However, here the system can exhibit the features of OB in the absence of control field ($\Omega_c = 0$). This is different from the situation $\Omega_s = 0$, where no OB was realized due to the effect of Rydberg EIT (see Fig. 2). The reason is that when $\Omega_c = 0$, the atomic system reduces to a three-level V-type atom–light configuration for which a small nonzero absorption is expected (see Fig. 5), resulting in the hysteresis cycle effect.

Plotting the scaled feedback output field versus the scaled input probe field in Fig. 6 demonstrates that OB can be switched to OM or vice versa by manipulating the switching field detuning Δ_s. It should be pointed out that unlike the OB, the output intensity has now more than two stable states at a given input, which makes the OM suitable for building multi-stable switching or coding elements.

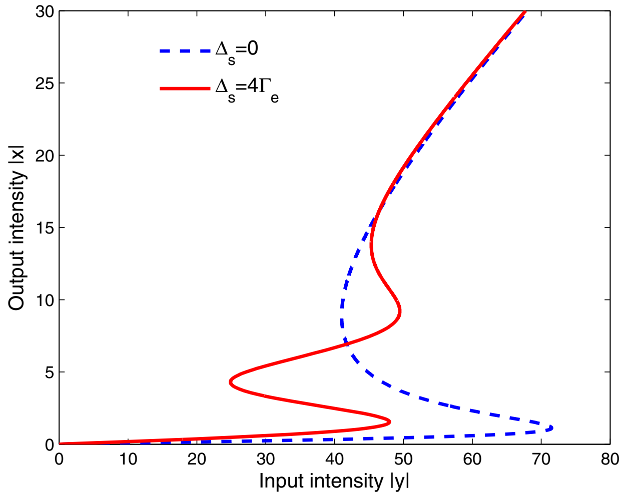

Fig. 6. Plots of the input–output field curves for different values of Δ_s. Here, $\Omega_c = \Omega_s = 3\Gamma_e$ and the other parameters are the same as in Fig. 2.

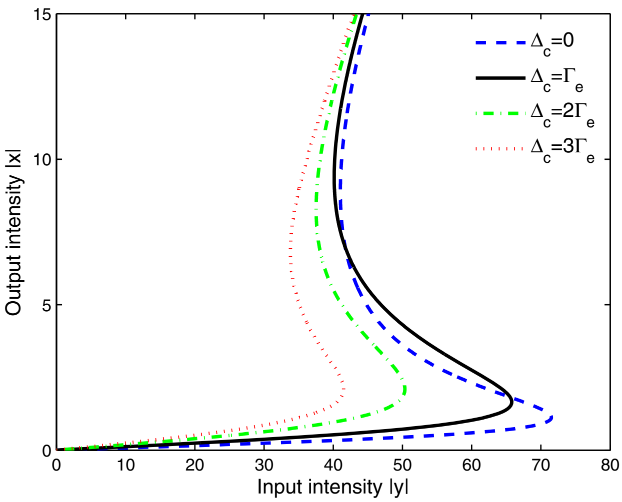

Fig. 7. Plots of the input–output field curves for different values of Δ_c. Here, $\Omega_c = \Omega_s = 3\Gamma_e$ and the other parameters are the same as in Fig. 2.

In order to find out how the bistable threshold intensity varies with the control field detuning Δ_c, we have plotted in Fig. 7 the input–output field curves for different values of Δ_c. One can see that the threshold and the hysteresis cycle shape are sensitive to the frequency detuning of the control field. To be more specific, increasing Δ_c leads to the reduction of OB threshold through modifying the absorption and nonlinearity of the atomic medium.

Next we explore the effect of the cooperation parameter $C = N\omega_p L|\mu_{eg}|^2/2\hbar\varepsilon_0 cT$ on the bistable behavior of the system. It is clear that the cooperation parameter C is directly proportional to the atomic number density. As shown in Fig. 8, OB tends to disappear for the small values of C when the atomic number density in the sample is small. Figure 8 also implies that the larger the C, the larger the OB threshold,

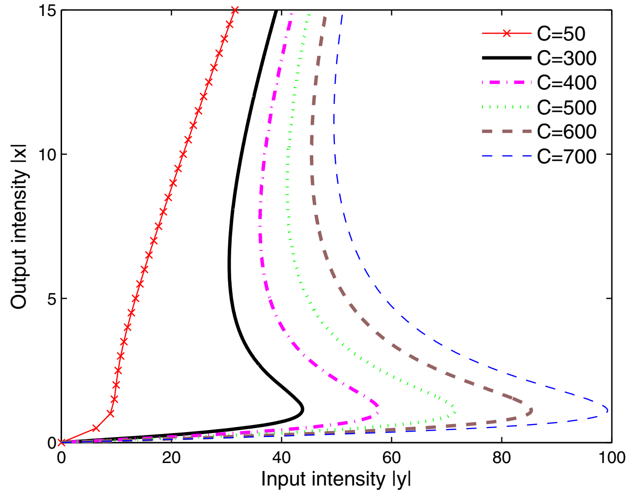

Fig. 8. Plots of the input–output field curves for different values of C. Here, $\Omega_c = \Omega_s = 3\Gamma_e$ and the other parameters are the same as in Fig. 2.

and hence, the stronger the absorption of the probe field in the medium.

Last, we have considered the propagation of a probe pulse in a realistic system where the incident wave has a Gaussian profile, and its propagation is controlled by another coupling field of larger intensity, together with the switching field. The propagation dynamics of the probe pulse through the medium and along the z direction are described by the Maxwell wave equation, which can be expressed as in the slowly varying envelope approximation

$$\frac{\partial\Omega_p(z,t)}{\partial z} + \frac{1}{c}\frac{\partial\Omega_p(z,t)}{\partial t} = ik\rho_{eg}(z,t), \tag{7}$$

where $k = \frac{N\omega_p|\mu_{eg}|^2}{4c\hbar\varepsilon_0}$ characterizes the strength light coupling with the atomic medium. Going to the retarded coordinates $\xi = z$ and $\tau = z - t/c$, we shall consider the propagation of a Gaussian-shaped probe pulse of the form

$$\Omega_p(0,\tau) = \Omega_p^0 e^{-[(\tau-\tau_0)/\sigma]^2}, \tag{8}$$

where Ω_p^0 is a real-valued constant describing the peak value of the Rabi frequency before the probe pulse enters the medium, τ_0 gives the peaks location, and σ denotes the temporal width of the input pulse.

Figure 9 demonstrates the propagation of a Gaussian pulse through the four-level atom–light coupling setup involving a Rydberg-state excitation. As illustrated in Fig. 9(a), without the switching field ($\Omega_s = 0$), the probe pulse does not experience the losses because of the Rydberg EIT. Turning on the switching field Ω_s, the system transforms from the Rydberg EIT to the Rydberg EIA. Setting $\Omega_s = \Omega_c$, the weak probe pulse propagates with the maximum losses inside the medium, as can be seen in Fig. 9(b). Thus, the medium acts as an absorptive optical switch in which the absorption of the probe pulse can be turned on and off by manipulating the coupling field Ω_s. This allows one to control the optical bistability, as shown in Fig. 2.

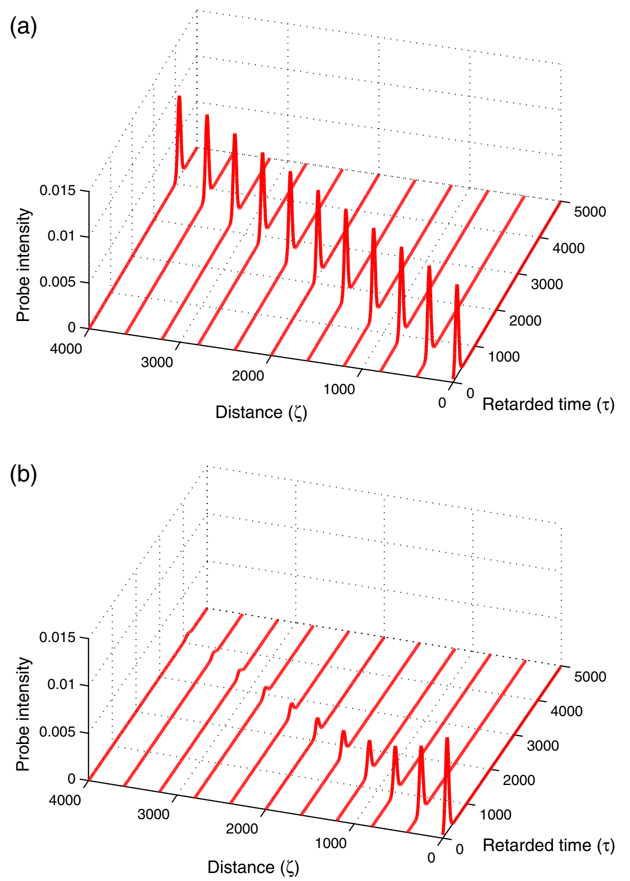

Fig. 9. Plots of probe field intensity in the medium against retarded time and distance for $\sigma = 70/\Gamma_e$, $\tau_0 = 180/\Gamma_e$, and (a) $\Omega_s = 0$, (b) $\Omega_s = 3\Gamma_e$. Here, $\Delta_p = 0$ and the other parameters are the same as in Fig. 3.

4. CONCLUSIONS

We have considered the optical bistability and multistability behaviors in a four-level atomic medium involving a Rydberg state immersed in a unidirectional ring cavity. The effects of the system parameters on the input–output properties of the probe field are explored. It is found that OB does not appear when the switching field is not introduced on the transition $|s\rangle \leftrightarrow |g\rangle$. We have attributed this to the Rydberg transparency of the resonant medium when $\Omega_s = 0$. However, Rydberg EIA becomes dominant once the switching field is turned on. We have shown that OB appears in the atomic scheme thanks to the Rydberg EIA. The OB threshold can be controlled using both control and switching field intensities. The possibility of switching between OB and OM has also been investigated.

Funding. Center for International Scientific Studies & Collaborations (CISSC), Islamic Republic of Iran; Lithuanian Research Council (VP1-3.1-ŠMM-01-V-03-001).

Acknowledgment. This work has been supported by the Center for International Scientific Studies & Collaborations (CISSC), Islamic Republic of Iran. H. R. Hamedi also gratefully acknowledges the support of the Lithuanian Research Council.

REFERENCES

1. L. V. Hau, S. E. Harris, Z. Dutton, and C. H. Behroozi, "Light speed reduction to 17 metres per second in an ultracold atomic gas," Nature **397**, 594–598 (1999).
2. Y. Wu and X. Yang, "Electromagnetically induced transparency in V-, Λ-, and cascade-type schemes beyond steady-state analysis," Phys. Rev. A **71**, 053806 (2005).
3. S. E. Harris, "Electromagnetically induced transparency," Phys. Today **50**(7), 36–42 (1997).
4. M. Fleischhauer, A. Imamoglu, and J. P. Marangos, "Electromagnetically induced transparency: optics in coherent media," Rev. Mod. Phys. **77**, 633–673 (2005).
5. M. Fleischhauer and M. D. Lukin, "Dark-state polaritons in electromagnetically induced transparency," Phys. Rev. Lett. **84**, 5094–5097 (2000).
6. M. S. Bigelow, N. N. Lepeshkin, and R. W. Boyd, "Observation of ultraslow light propagation in a ruby crystal at room temperature," Phys. Rev. Lett. **90**, 113903 (2003).
7. M. D. Lukin, "Colloquium: trapping and manipulating photon states in atomic ensembles," Rev. Mod. Phys. **75**, 457–472 (2003).
8. M. Sahrai, H. Tajalli, K. T. Kapale, and M. S. Zubairy, "Tunable phase control for subluminal to superluminal light propagation," Phys. Rev. A **70**, 023813 (2004).
9. S.-M. Ma, H. Xu, and B. S. Ham, "Electromagnetically-induced transparency and slow light in GaAs/AlGaAs multiple quantum wells in a transient regime," Opt. Express **17**, 14902–14908 (2009).
10. J. Xu and X.-M. Hu, "Sub-half-wavelength localization of an atom via trichromatic phase control," J. Phys. B **40**, 1451–1459 (2007).
11. H.-T. Zhang, H. Wang, and Z.-P. Wang, "Two-dimensional atom localization via two standing-wave fields in a four-level atomic system," Phys. Scripta **84**, 065402 (2011).
12. J. Li, R. Yu, M. Liu, C. Ding, and X. Yang, "Efficient two-dimensional atom localization via phase-sensitive absorption spectrum in a radio-frequency-driven four-level atomic system," Phys. Lett. A **375**, 3978–3985 (2011).
13. Z. Wang, T. Shui, and B. Yu, "Efficient two-dimensional atom localization in a four-level atomic system beyond weak-probe approximation," Opt. Commun. **313**, 263–269 (2014).
14. Z. Wang and B. Yu, "High-precision two-dimensional atom localization via quantum interference in a tripod-type system," Laser Phys. Lett. **11**, 035201 (2014).
15. J. Xu, Q. Li, W.-C. Yan, X.-D. Chen, and X.-M. Hu, "Sub-half-wavelength localization of a two-level atom via trichromatic phase manipulation," Phys. Lett. A **372**, 6032–6036 (2008).
16. C. Ding, J. Li, X. Yang, Z. Zhan, and J.-B. Liu, "Two-dimensional atom localization via a coherence-controlled absorption spectrum in an N-tripod-type five-level atomic system," J. Phys. B **44**, 145501 (2011).
17. X. X. Yang, Z. W. Li, and Y. Wu, "Four-wave mixing via electron spin coherence in a quantum well waveguide," Phys. Lett. A **340**, 320–325 (2005).
18. Y. Wu, J. Saldana, and Y. Zhu, "Large enhancement of four-wave mixing by suppression of photon absorption from electromagnetically induced transparency," Phys. Rev. A **67**, 013811 (2003).
19. G. Wang, Y. Xue, C.-L. Cui, Y. Qu, and J.-Y. Gao, "Highly efficient four-wave mixing induced by quantum constructive interference in rubidium vapour," Chin. Phys. B **21**, 034205 (2012).
20. Y. Zhang, B. Anderson, and M. Xiao, "Energy transfer between four-wave and six-wave mixing processes in rubidium atoms via atomic coherence," Phys. Rev. A **77**, 061801 (2008).
21. H. R. Hamedi, A. H. Gharamaleki, and M. Sahrai, "Colossal Kerr nonlinearity based on electromagnetically induced transparency in a five-level double-ladder atomic system," Appl. Opt. **55**, 5892–5899 (2016).
22. C. Zhu and G. Huang, "Giant Kerr nonlinearity, controlled entangled photons and polarization phase gates in coupled quantum-well structures," Opt. Express **19**, 23364–23376 (2011).
23. Y. Wu and X. Yang, "Giant Kerr nonlinearities and solitons in a crystal of molecular magnets," Appl. Phys. Lett. **91**, 094104 (2007).
24. H. R. Hamedi and G. Juzeliūnas, "Phase-sensitive Kerr nonlinearity for closed-loop quantum systems," Phys. Rev. A **91**, 053823 (2015).
25. J. Sheng, X. Yang, H. Wu, and M. Xiao, "Modified self-Kerr-nonlinearity in a four-level N-type atomic system," Phys. Rev. A **84**, 053820 (2011).

26. C. Hang and G. Huang, “Giant Kerr nonlinearity and weak-light superluminal optical solitons in a four-state atomic system with gain doublet,” Opt. Express **18**, 2952–2966 (2010).
27. Y. Niu and S. Gong, “Enhancing Kerr nonlinearity via spontaneously generated coherence,” Phys. Rev. A **73**, 053811 (2006).
28. H. Wang, D. Goorskey, and M. Xiao, “Dependence of enhanced Kerr nonlinearity on coupling power in a three-level atomic system,” Opt. Lett. **27**, 258–260 (2002).
29. Y. Wu, “Two-color ultraslow optical solitons via four-wave mixing in cold-atom media,” Phys. Rev. A **71**, 053820 (2005).
30. L.-G. Si, W.-X. Yang, X.-Y. Lü, X. Hao, and X. Yang, “Formation and propagation of ultraslow three-wave-vector optical solitons in a cold seven-level triple-Λ atomic system under Raman excitation,” Phys. Rev. A **82**, 013836 (2010).
31. W.-X. Yang, A.-X. Chen, R.-K. Lee, and Y. Wu, “Matched slow optical soliton pairs via biexciton coherence in quantum dots,” Phys. Rev. A **84**, 013835 (2011).
32. Y. Wu, “Matched soliton pairs of four-wave mixing in molecular magnets,” J. Appl. Phys. **103**, 104903 (2008).
33. Y. Wu and L. Deng, “Ultraslow optical solitons in a cold four-state medium,” Phys. Rev. Lett. **93**, 143904 (2004).
34. Y. Chen, Z. Bai, and G. Huang, “Ultraslow optical solitons and their storage and retrieval in an ultracold ladder-type atomic system,” Phys. Rev. A **89**, 023835 (2014).
35. J.-H. Li, X.-Y. Lü, J.-M. Luo, and Q.-J. Huang, “Optical bistability and multistability via atomic coherence in an N-type atomic medium,” Phys. Rev. A **74**, 035801 (2006).
36. H. R. Hamedi, “Optical bistability and multistability via magnetic field intensities in a solid,” Appl. Opt. **53**, 5391–5397 (2014).
37. J. Li, “Coherent control of optical bistability in a microwave-driven V-type atomic system,” Phys. D **228**, 148–152 (2007).
38. Z. Wang, A.-X. Chen, Y. Bai, W.-X. Yang, and R.-K. Lee, “Coherent control of optical bistability in an open Λ-type three-level atomic system,” J. Opt. Soc. Am. B **29**, 2891–2896 (2012).
39. Z. Wang and B. Yu, “Optical bistability and multistability via dual electromagnetically induced transparency windows,” J. Lumin. **132**, 2452–2455 (2012).
40. A. Joshi, A. Brown, H. Wang, and M. Xiao, “Controlling optical bistability in a three-level atomic system,” Phys. Rev. A **67**, 041801(R) (2003).
41. D. Zhang, J. Li, C. Ding, and X. Yang, “Control of optical bistability via an elliptically polarized light in a four-level tripod atomic system,” Phys. Scr. **85**, 035401 (2012).
42. J. Yuan, W. Feng, P. Li, X. Zhang, Y. Zhang, H. Zheng, and Y. Zhang, “Controllable vacuum Rabi splitting and optical bistability of multi-wave-mixing signal inside a ring cavity,” Phys. Rev. A **86**, 063820 (2012).
43. Z. Zhang, H. Chen, L. Zhang, D. Zhang, X. Li, Y. Zhang, and Y. Zhang, “Unveiling the relationship between optical bistability and vacuum Rabi splitting,” Europhys. Lett. **117**, 53001 (2017).
44. M. Soljacic, E. Lidorikis, M. Ibanescu, S. G. Johnson, J. D. Joannopoulos, and Y. Fink, “Optical bistability and cutoff solitons in photonic bandgap fibers,” Opt. Express **12**, 1518–1527 (2004).
45. J.-H. Li, “Controllable optical bistability in a four-subband semiconductor quantum well system,” Phys. Rev. B **75**, 155329 (2007).
46. J. Li, X. Hao, J. Liu, and X. Yang, “Optical bistability in a triple semiconductor quantum well structure with tunnelling-induced interference,” Phys. Lett. A **372**, 716–720 (2008).
47. J.-H. Li, “Coherent control of optical bistability in tunnel-coupled double quantum wells,” Opt. Commun. **274**, 366–371 (2007).
48. L. Li, H. Zhang, H. Sun, X. Hu, W. Liu, and X. Yi, “Tunneling-induced optical bistability in an asymmetric double quantum well,” Appl. Opt. **55**, 2980–2984 (2016).
49. B. S. Ham, P. R. Hemmer, and M. S. Shahriar, “Efficient electromagnetically induced transparency in a rare-earth-doped crystal,” Opt. Commun. **144**, 227–230 (1997).
50. J. J. Longdell, E. Fraval, M. J. Sellars, and N. B. Manson, “Stopped light with storage times greater than one second using electromagnetically induced transparency in a solid,” Phys. Rev. Lett. **95**, 063601 (2005).
51. H.-F. Zhang, J.-H. Wu, X.-M. Su, and J.-Y. Gao, “Quantum-interference effects on the index of refraction in an Er^{3+}-doped yttrium aluminum garnet crystal,” Phys. Rev. A **66**, 053816 (2002).
52. Z. Wang, B. Yu, S. Zhen, X. Wu, J. Zhu, and Z. Cao, “Controllable optical bistability and multistability in a rare-earth-ion-doped optical fiber,” Superlattices Microstruct. **51**, 324–331 (2012).
53. C. Li, Z. Jiang, Y. Zhang, Z. Zhang, F. Wen, H. Chen, Y. Zhang, and M. Xiao, “Controlled correlation and squeezing in $Pr^{3+}:Y_2SiO_2$ to yield correlated light beams,” Phys. Rev. Appl. **7**, 014023 (2017).
54. T. F. Gallagher, *Rydberg Atoms* (Cambridge University, 1994).
55. M. Saffman, T. G. Walker, and K. Mølmer, “Quantum information with Rydberg atoms,” Rev. Mod. Phys. **82**, 2313–2363 (2010).
56. M. G. Bason, M. Tanasittikosol, A. Sargsyan, A. K. Mohapatra, D. Sarkisyan, R. M. Potvliege, and C. S. Adams, “Enhanced electric field sensitivity of rf-dressed Rydberg dark states,” New J. Phys. **12**, 065015 (2010).
57. T. A. Johnson, E. Urban, T. Henage, L. Isenhower, D. D. Yavuz, T. G. Walker, and M. Saffman, “Rabi oscillations between ground and Rydberg states with dipole-dipole atomic interactions,” Phys. Rev. Lett. **100**, 113003 (2008).
58. A. K. Mohapatra, T. R. Jackson, and C. S. Adams, “Coherent optical detection of highly excited Rydberg states using electromagnetically induced transparency,” Phys. Rev. Lett. **98**, 113003 (2007).
59. J. D. Pritchard, D. Maxwell, A. Gauguet, K. J. Weatherill, M. P. A. Jones, and C. S. Adams, “Cooperative atom–light interaction in a blockaded Rydberg ensemble,” Phys. Rev. Lett. **105**, 193603 (2010).
60. P. Bohlouli-Zanjani, J. A. Petrus, and J. D. D. Martin, “Enhancement of Rydberg atom interactions using AC stark shifts,” Phys. Rev. Lett. **98**, 203005 (2007).
61. D. Petrosyan, J. Otterbach, and M. Fleischhauer, “Electromagnetically induced transparency with Rydberg atoms,” Phys. Rev. Lett. **107**, 213601 (2011).
62. J. Ruseckas, I. A. Yu, and G. Juzeliūnas, “Creation of two-photon states via interactions between Rydberg atoms during light storage,” Phys. Rev. A **95**, 023807 (2017).
63. C. Carr, M. Tanasittikosol, A. Sargsyan, D. Sarkisyan, C. S. Adams, and K. J. Weatherill, “Three-photon electromagnetically induced transparency using Rydberg states,” Opt. Lett. **37**, 3858–3860 (2012).
64. Z. Zhang, H. Zheng, X. Yao, Y. Tian, J. Che, X. Wang, D. Zhu, Y. Zhang, and M. Xiao, “Phase modulation in Rydberg dressed multi-wave mixing processes,” Sci. Rep. **5**, 10462 (2015).
65. V. Bharti and V. Natarajan, “Sub- and super-luminal light propagation using a Rydberg state,” Opt. Commun. **392**, 180–184 (2017).
66. V. Bharti, A. Wasan, and V. Natarajan, “Wavelength mismatch effect in electromagnetically induced absorption,” Phys. Lett. A **380**, 2390–2394 (2016).
67. V. Bharti and V. Natarajan, “Study of a four-level system in vee + ladder configuration,” Opt. Commun. **356**, 510–514 (2015).
68. R. Bonifacio and L. A. Lugiato, “Optical bistability and cooperative effects in resonance fluorescence,” Phys. Rev. A **18**, 1129–1144 (1978).